2023 IEEE International Conference on Robotics and Automation (ICRA 2023)
May 29 - June 2, 2023. London, UK

# Robot Trust and Self-Confidence Based Role Arbitration Method for Physical Human-Robot Collaboration

Qiao Wang[1], Dikai Liu[1], Marc G. Carmichael[1], and Chin-Teng Lin[2]

***Abstract*— Role arbitration in human-robot collaboration (HRC) is a dynamically changing process that is affected by many factors such as physical workload, environmental changes and trust. In order to address this dynamic process, a trust-based role arbitration method is studied in this research. A computational model of robot trust and self-confidence (TSC) in physical human-robot collaboration (pHRC) is proposed. The TSC model is defined as a function of objective robot and human co-worker performance. A role arbitration method is then proposed based on the TSC model presented. The human-in-the-loop experiments with a collaborative robot are conducted to verify the TSC-based role arbitration method. The results show that the proposed method could achieve superior human-robot combined performance, reduce human co-workers' workload, and improve subjective preference.**

## I. INTRODUCTION

The emergence of collaborative robots (cobots) allows humans and robots to work in the same space. The strengths of humans (e.g. perception and decision-making) and robots (e.g. repeatability and accuracy) are combined to achieve better performance. Human co-workers could interact with a robot in various ways. In this paper, we focus on physical Human-Robot Collaboration (pHRC). pHRC can be defined as a human co-worker physically contacts or exchanges force continuously with a robot to accomplish a shared goal in the same workspace. pHRC can be applied in various applications, such as rehabilitation and material handling [1], [2]. One pHRC scenario is shown in Figure 1.

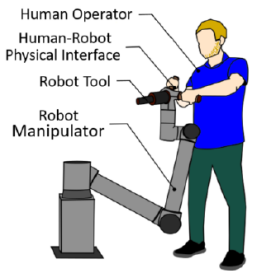


Fig. 1. A pHRC scenario with a human co-worker physically collaborating with a robot manipulator [3]

Role arbitration in pHRC refers to how the control is allocated between humans and robots for a task and allows combining the strengths of humans and robots to improve combined performance and reduce human physical or cognitive effort [4].

The willingness of a human to rely on the robot taking control during pHRC depends on the difference between the human's trust in the robot and the human's trust in themselves to perform the task [5]. The robot can take control when human trust in the robot is higher than trusting themselves, otherwise, the human is in control. Saeidi [6] proposed a human trust in robot and self-confidence model and a control switching method for the (semi)autonomous mobile robotic systems. Saeidi [7] also proposed a mixed-initiative method that is based on human trust in robots.

The human co-worker's interaction experience with robots is one of the critical aspects of pHRC due to the constant physical contact between the human and the robot [8]. The aforementioned trust-based role allocation strategies are based on human-to-robot trust [6], [7]. Wang [9] developed a computational model for robot trust in human co-workers in pHRC. To emulate the human control allocation process, we want the robot to act as an active partner, i.e. a peer. Therefore, we develop a human-preferred role arbitration method based on robot-to-human trust and robot self-confidence (TSC).

The proposed TSC model is defined as the difference between robot-to-human trust and the robot's self-confidence. Robot-to-human trust model developed in [9] is used in this research. This model takes into account safety, robot singularity, smoothness, physical performance and cognitive performance. The robot's self-confidence is modelled based on whether a human agrees with the control actions of the robot. The robot's self-confidence is high when a human agrees with robot control and vice versa. In addition, when the robot's trust in a human co-worker is much higher than the robot's self-confidence, the control is allocated to the human co-worker and vice versa. However, the way the control is allocated when the robot's trust in human co-workers and itself are both high or low becomes a question. In this case, the history of robot self-confidence can be used. If the robot's self-confidence in history is high, it indicates that the robot control was satisfied by the human in the past. Hence, the control will be biased toward the robot and vice versa.

Therefore, we proposed a TSC-based role arbitration method. It is shown through experimental analysis that this method can achieve superior human-robot combined performance, reduce human co-workers' workload, and improve subjective preference. The control system for role arbitration

[1]Qiao Wang, Dikai Liu and Marc G. Carmichael are with the Robotics Institute, Faculty of Engineering and Information Technology, University of Technology Sydney, 81 Broadway, Ultimo NSW 2010, Australia {Qiao.Wang-1}@student.uts.edu.au;

[2] Chin-Teng Lin is with the Australian Artificial Intelligence Institute, School of Computer Science, Faculty of Engineering and Information Technology, University of Technology Sydney, 81 Broadway, Ultimo NSW 2010, Australia

method is presented in Section II. The computational TSC model is described in Section III. The TSC-based role arbitration method is shown in Section IV. An experimental testbed and design of experiments are presented in Section V. The results and discussion are shown in Section VI, and the conclusion and future work are in Section VII.

## II. CONTROL SYSTEM

Evrard [10] proposed an idea that could switch continuously between two distinct behaviours (follower and leader) for the robot in pHRC. Hence, a control scheme is proposed that consists of both follower and leader roles of the robot as shown in Equation 1. The roles (follower and leader) of the robot is adapted by a role arbitration function $\alpha \in [0, 1]$ which will be explained in Section IV. The human or the robot acts as a leader role (i.e. in control) when $\alpha = 0$ or $\alpha = 1$.

$$\dot{x} = \dot{x}_H + \alpha \dot{x}_R \tag{1}$$

$\dot{x}$ is the velocity command sent to the robot manipulator. $\dot{x}_H$ is the human control and $\dot{x}_R$ is the robot control.

The follower role of the robot is achieved through an admittance control so that the robot could move based on the force, $F_H$, applied by the human co-worker when the human is in control (the leader, $\alpha = 0$) which is shown as:

$$M_d \ddot{x}_H + D_d \dot{x}_H = F_H \tag{2}$$

$M_d$ and $D_d$ are the desired robot inertia and damping matrix. $x_H$ is the desired pose of the end-effector in the Cartesian space. $F_H$ is the external force applied on the robot end-effector by a human co-worker. When the robot is leader ($\alpha = 1$), a bounded impedance control model is employed inspired by [11]:

$$\dot{x}_R = min(\dot{x}_{max}, \dot{x}_{max} \frac{d}{d_{th}}) \tag{3}$$

$d$ is the distance between the desired and the current end-effector position. $\dot{x}_{max}$ is the maximum robot velocity. $d_{th}$ is the threshold distance when the robot control $\dot{x}_R$ reaches $\dot{x}_{max}$, i.e. $d = d_{th}$. The bounded $\dot{x}_R$ helps to improve the safety of human co-workers and interaction experiences during pHRC due to the physical couplings of the human-robot system [11]. Hence, $\dot{x}_{max}$ should be designed to ensure safety and acceptable interaction experience. Also, $\dot{x}_{max}$ should be large enough to ensure the robot acting as a leader when $\alpha = 1$.

## III. ROBOT TRUST IN HUMAN CO-WORKER AND ROBOT SELF-CONFIDENCE MODEL

The willingness of a human to rely on the robot taking control depends on the difference between the human-to-robot trust and the human's self-confidence to perform the task [5]. Hence, a similar control allocation process is proposed. The robot's reliance on a human co-worker taking control depends on the difference between robot-to-human trust and the robot's self-confidence. The robot-to-human trust reflects the capability, from the robot's perspective, of human co-workers to take control during pHRC. The robot's self-confidence reflects the capability of the robot to take control. Therefore, a real-time computational model of the difference between robot-to-human trust $T \in [0, 1]$ and robot's self-confidence $SC \in [0, 1]$ at time step $n$ can be simply defined as:

$$TSC[n] = T[n] - SC[n] \tag{4}$$

$TSC$ is bounded between -1 and 1. $T$ and $SC$ will be introduced in Section III-A and III-B, respectively.

### A. Robot Trust in Human Co-worker ($T$)

The trust of humans in robots is dynamic and highly depends on the robot performance [12]. Similarly, the robot trust in its human co-worker can be assumed and modelled as the performance of the human co-worker [9]:

$$T[n] = \frac{\sum_{k=0}^{N_1} \beta_1^k p_H[n-k]}{\sum_{k=0}^{N_1} \beta_1^k} \tag{5}$$

$T \in [0, 1]$ is the robot's trust in a human co-worker. $T = 0$ (or $T = 1$) represents no trust (or full trust) in the human co-worker. $p_H \in [0, 1]$ is a normalised measure of human performance. A discount factor $\beta_1 \in [0, 1]$ is introduced to reduce sensitivity to historic performance as more recent performance has greater impact on trust [13]. $\beta_1^k$ is the weighting of $p_H$ at the time step $n - k$. $N_1$ is the length of the moving time window and $n$ is the current time step. $p_H$ is modelled by important pHRC factors, including safety $p_S$, singularity $p_{SP}$, smoothness $p_{SM}$, physical $p_{PW}$ and cognitive performance $p_{CW}$ [9].

$$p_H[n] = p_S p_{SP}(C + (1-C)(\gamma_{SM} p_{SM} + \gamma_{PW} p_{PW} + \gamma_{CP} p_{CP})) \tag{6}$$

The weighting coefficients $\gamma_{SM} + \gamma_{PW} + \gamma_{CP} = 1$ are positive constants that could be adjusted based on the relative importance of the corresponding factors according to specific task requirements. $C$ represents the maximum contribution of $p_{SM}$, $p_{PW}$ and $p_{CW}$.

### B. Robot Self-Confidence ($SC$)

Robot self-confidence $SC \in [0, 1]$ is the robot trust in itself. Similar to Equation 5 the robot self-confidence is defined as:

$$SC[n] = \frac{\sum_{k=0}^{N_2} \beta_2^k p_R[n-k]}{\sum_{k=0}^{N_2} \beta_2^k} \tag{7}$$

$\beta_2$ and $N_2$ are similar to $\beta_1$ and $N_1$ which have been explained in Section III-A. The robot performance $p_R$ is defined as the level of the agreement of the human co-worker on the control action of the robot $\dot{x}_R$. There are scenarios, such as a human co-worker changing a task plan, accumulation of sensor noise, or unexpected obstacles that will result in the robot not accomplishing the pre-programmed task by itself or does not behave as the human co-worker expected. This will result in the level of agreement on $\dot{x}_R$ being low, which leads to $p_R$ being low and vice versa.

$p_R$ is modelled as a function of the difference between human control $\dot{x}_H$ and robot control $\dot{x}_R$ as shown in Equation 8. When the difference between those two controls is

too significant, and the two control directions are opposite, it indicates that the level of agreement with $\dot{x}_R$ is low. If those two controls are in the same direction, it indicates that the human co-worker agrees with the $\dot{x}_R$. Therefore, the difference between those two controls $V_D$ is shown as:

$$V_D[n] = \begin{cases} |\dot{x}_H - \dot{x}_R| & \text{if } sign(\dot{x}_H) \neq sign(\dot{x}_r) \\ 0 & \text{Otherwise} \end{cases} \quad (8)$$

A single timestep $V_D$ may not represent the actual human co-worker intention because human co-workers may unintentionally apply a force in the opposite direction or a large force due to uncertainty of human motor movement. Therefore, the moving averaged method is employed as shown in Equation 9. Hence, the averaged difference $M_{V_D}$ is calculated by:

$$M_{V_D}[n] = \frac{1}{W_r} \sum_{i=n-w_r+1}^{n} V_D[i] \quad (9)$$

$W_r$ is the time window that determines the sensitivity of $M_{V_D}$ on $V_D$. If $W_r$ is small, $M_{V_D}$ may be sensitive to the random movement of a human co-worker. If $W_r$ is large, a human co-worker needs to apply additional force (Equation 2) to signal the disagreement. Robot performance $p_R$ is then defined as:

$$p_R = \begin{cases} 1 & M_{V_D} \leq M^-_{V_D} \\ \frac{M^+_{V_D} - M_{V_D}}{M^+_{V_D} - M^-_{V_D}} & M^-_{V_D} < M_{V_D} < M^+_{V_D} \\ 0 & M_{V_D} \geq M^+_{V_D} \end{cases} \quad (10)$$

$M^+_{V_D}$ and $M^-_{V_D}$ are the two thresholds of $M_{V_D}$. When $M_{V_D} \leq M^-_{V_D}$, $M_{V_D}$ is small indicating the human co-worker agrees with $\dot{x}_R$ so that $p_R$ is high ($p_R = 1$) and vice versa. When the values of $M^+_{V_D}$ and $M^-_{V_D}$ are large, the human co-worker will be required to put more physical effort in order to take control of the robot. The advantage is that the robot control will not be easily affected by accidental human movement. Furthermore, when those values are small, the control is easily shifted toward the human co-worker. However, robot control can be easily affected by unintentional human movement.

## IV. A Robot Trust and Self-Confidence Based Role Arbitration Method ($\alpha$)

Saedi [7] proposed a TSC-based control allocation method for mobile robot. However, a step-like arbitration function was proposed, which is not appropriate in pHRC because human comfort will be significantly affected when the control authority is shifted suddenly [3].

A novel smooth role arbitration function $\alpha(TSC)$ is proposed. A fifth-order polynomial equation (Figure 2) is proposed with null first and second derivatives at the $TSC^-$, and $TSC^+$, which is inspired by [14]. Hence, the role arbitration function $\alpha(TSC)$ is defined as a function of $TSC$:

$$\alpha(TSC) = \begin{cases} 1 & TSC \leq TSC^- \\ 0 & TSC \geq TSC^+ \\ aTSC^5 + bTSC^4 + cTSC^3 & \\ +dTSC^2 + eTSC + f & \text{Otherwise} \end{cases} \quad (11)$$

$TSC^-$ and $TSC^+$ are the thresholds determining whether the robot is acting as an leader ($\alpha = 1$ when $TSC <= TSC^-$) or follower ($\alpha = 0$ when $TSC >= TSC^+$). When the robot trust in human is much larger than trusting in itself ($T >> SC$), $TSC$ is large ($TSC >= TSC^+$ based on Equation 4). The robot reliance on human is high and act as a follower ($\alpha = 0$) and vice versa.

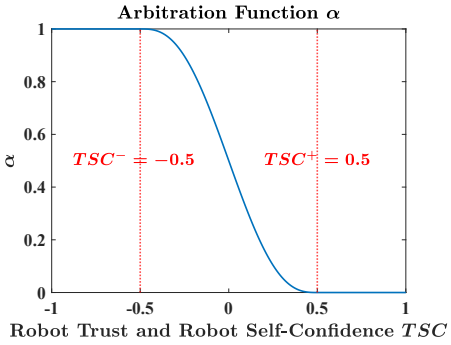


Fig. 2. Examples of the arbitration function $\alpha$ (Equation 11) $TSC^- = -0.5$, $TSC^+ = 0.5$, $a = -6$, $b = 0$, $c = 5$, $d = 0$, $e = -1.875$ and $f = 0.5$.

A dilemma arises when robot trust in human co-worker and robot trust in itself are both high or low (When both $T$ and $SC$ approach 1 or 0) resulting in the difference between them approaches 0 ($TSC \rightarrow 0$) from Equation 4. The role allocation has not been addressed yet.

Hence, we proposed a method to address this problem. As it can be seen from the example shown in Figure 2, when $TSC^- = -0.5$ and $TSC^+ = 0.5$, $\alpha(TSC = 0) = 0.5$. When $TSC^-$ and $TSC^+$ are smaller, the control is biased toward human co-workers ($\alpha$ is smaller) and vice versa when $TSC \approx 0$. Therefore, instead of estimating a fixed value of $TSC^-$ and $TSC^+$ heuristically, dynamic equations (Equation 12) are developed for adapting $TSC^+ \in [0, 1]$ and $TSC^- \in [-1, 0]$ based on the history of human agreement with the robot control $\dot{x}_R$ to address different levels of robot's capability in accomplishing the task by itself. If $\dot{x}_R$ consistently mismatch human intention ($SC$ is low from Equation 10), this represents that the robot cannot accomplish the task by itself. As a result, $TSC^+$ and $TSC^-$ will converge to 0 and -1, $\alpha \rightarrow 0$ when $TSC$ is close to 0 to ensure the human leader role. If $\dot{x}_R$ consistently matches human intention ($SC$ is high), the robot should take the leader role to maximize the combined performance and reduce human co-worker workload due to the robot's inherent advantage in speed, accuracy, and power. Correspondingly, $TSC^+$ and $TSC^-$ will gradually increase and converge to 1 and 0 so

that $\alpha \rightarrow 1$ when $TSC \approx 0$.

$$\begin{cases} \dot{TSC^+} = \frac{1}{\tau}(SC - TSC^+) \\ \dot{TSC^-} = \frac{1}{\tau}(SC - TSC^-) \\ TSC^- = TSC^- - 1 \end{cases} \tag{12}$$

$\tau$ is the time constant which determines the sensitivity of $\dot{TSC^+}$ and $\dot{TSC^-}$ to $SC$. When $\tau$ is larger, the variation of $TSC^+$ and $TSC^-$ will be smaller and vice versa.

Based on the trials on the actual robot, it was found that control authority shifts from robot to human ($\alpha : 1 \rightarrow 0$) instantaneously which is desirable and intuitive for a human co-worker. If the control authority is shifted too slowly, the human co-worker will likely feel that the robot is uncontrollable. However, smooth and continuous control shifting is desirable from the human co-worker to the robot ($\alpha : 0 \rightarrow 1$). Abrupt control shifting will significantly affect the human's perception [3]. Hence, $\alpha$ is constrained as:

$$\alpha[n] = \begin{cases} \alpha[n-1] + \frac{1}{\text{rate} \times \tau_r} & \alpha[n] - \alpha[n-1] > \frac{1}{\text{rate} \times \tau_r} \\ \alpha[n] & \text{otherwise} \end{cases} \tag{13}$$

$rate$ is the sampling rate of the system. $\tau_r$ is the minimum time taken for role arbitration between $\alpha = 1$ and $\alpha = 0$ which is individual-dependent. $\tau_r$ is suggested to be greater than 0.48 seconds because it is the fastest human response time [15].

## V. Experimental Evaluation

### A. Experiment Testbed

The experiment testbed used in this research is called ANBOT, as shown in Figure 3a. ANBOT consists of a UR10 arm and a six-axis force-torque sensor mounted between the robotic arm and robot end-effector to measure the human co-worker's interaction force. There is a monitor to display the actual trajectory of the robot end-effector, as shown in Figure 3b. In this experiment, the robot's movement is constrained into two dimensions to reduce the complexity of the experiment.

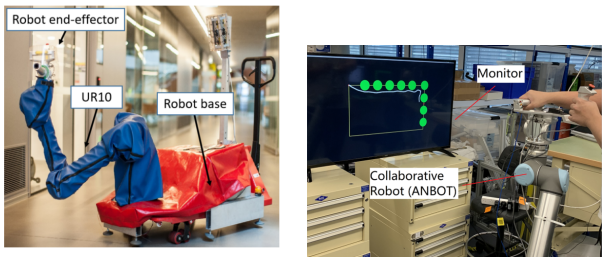


Fig. 3. (a) Experimental Testbed - ANBOT [16]. (b) The human co-worker operating the ANBOT follows the moving target. The detailed task scenario on the monitor is shown in Figure 4.

### B. Design of Experiments

A moving target (Red filled circle) tracking experiment is designed for verifying the proposed TSC-based role arbitration method as shown in Figure 4. In this experiment, a human co-worker is asked to move the robot end-effector to track the moving target and at the same time avoid collisions with the obstacles that are placed on the trajectory of the moving target. The experiment is considered a failure when the robot collides with obstacles. The moving target's position is known, but the obstacles' positions are not known by the robot.

In the safety performance model developed by Wang [9], the safety performance $p_S$ is defined as the possibility of colliding with the obstacles. In this experiment, $p_S$ is defined as the possibility of tracking with the desired moving target. As a result, when the possibility of tracking is high, $p_S$ is high. $a^- = 5cm/s^2, a^+ = 10cm/s^2$. Smoothness $p_{SM}$, physical $p_{PW}$ and cognitive performance $p_{CW}$ are not considered important in this experiment design, therefore, $C = 1$ in Equation 6. Also, the robot movement will always need to be in non-singular configurations during the experiment, so that $p_{SP} = 1$. The parameters of the control system presented in Section II are set as: $M_d = diag(5kg, 5kg)$, $D_d = diag(300Ns/m, 300Ns/m)$, $\dot{x}_{max} = 0.1m/s$, $d_{th} = 3cm$.

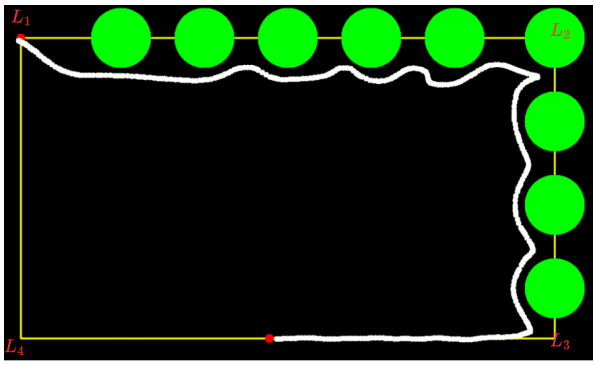


Fig. 4. The target (Red filled circle) starts from the top left corner and moves around the rectangle path (yellow line) in a clockwise direction with constant speed. When the moving target returns to the starting position, it is regarded as completing one experiment. The big filled green circles are the obstacles. The white line is the actual trajectory of the robot end-effector. L1, L2, L3 and L4 are the timestep when the moving target reaches four corners of the rectangle path.

### C. Three Control Strategies and Evaluations

For comparison of results, three control strategies are implemented in the experiments:

1) *HL*: Human in control $\alpha = 0$ (Equation 1)
2) *RL*: Robot in control $\alpha = 1$ (Equation 1)
3) *RA*: Robot Trust and Self-Confidence Based Role Arbitration Method. $\alpha(TSC)$

To evaluate the effectiveness of the proposed method, the following metrics are used:

1) *Average Magnitude of Human Force Over the Whole Trajectory*: $\frac{1}{Nc}\sum_0^{Nc}(\frac{1}{t_N - t_1}\sum_{t_1}^{t_N}||F_H(t)||)$. $Nc$ is the total number of experiments for the corresponding control strategies. $t_1$ is the initial timestep of the experiment. $t_N$ is the final timestep. $||F_H(t)||$ is the magnitude of human force at each timestep.

2) *Average Tracking Error Over the Whole Trajectory*: $\frac{1}{Nc}\sum_{0}^{Nc}(\frac{1}{t_N-t_1}\sum_{t_1}^{t_N}||e(t)||)$. $||e(t)||$ is the tracking error which is the distance between the position of the end-effector and the moving target at each timestep.
3) *Average Magnitude of Human Force at each timestep*: $\frac{1}{Nc}\sum_{0}^{Nc}||F_H(t)||$.
4) *Average Tracking Error at each timestep*: $\frac{1}{Nc}\sum_{0}^{Nc}||e(t)||$.
5) *Failure Rate*: $FR = \frac{\text{number of Failed experiments}}{\text{Total number of experiments}}$. Failure experiments refer to the situation when the robot collides with obstacles.
6) *NASA TLX*: Post-experiment questionnaires for measuring the perceived workload of the participants.

### D. Participants and Testing Procedure

Five participants are involved in the experiment. Four participants are from UTS Robotics Institute and one participant is from general public. The age is ranged between 25 and 35. After completing the consent form, each participant learns how to operate the ANBOT as shown in Figure 3a until they are familiar with the task. This is to reduce the learning effect. After these steps, each participant will undertake five trials for each control strategy in a random order to reduce the order effect. The participants are required to answer the questionnaires once they finish the experiments. This experiment follows the procedure approved by the UTS Ethical Committee with approval number ETH21-6346.

## VI. Results and Discussion

Figure 5 shows the mean and standard deviation of the human co-worker's average tracking error and magnitude of force (Metrics (1) and (2) in Section V-C) for each control strategy (HL, RA and RL) from all the five participants.

Figure 5 (a) and (b) present the resultant human force and tracking error over the Whole trajectory, i.e. from L1, L2, L3, L4 to L1. Figure 5 (c) and (d) present the resultant human force and tracking error over the first half of the trajectory with obstacles, i.e. from L1, L2 to L3. Figure 5 (e) and (f) present the resultant human force and tracking error over the second half of the trajectory without obstacles, i.e. from L3, L4 to L1.

Figure 6 shows the average human force and tracking error of the five participants at each timestep during the experiment (Metrics (3) and (4) in Section V-C).

### A. Average Magnitude of Human Force

*1) Over the Whole Trajectory:* Figure 5(a) shows that the RA control strategy can reduce the magnitude of human force by 40.7% and 37.6% compared to strategies of HL and RL, respectively.

*2) With obstacles (over the trajectory from L1, L2 to L3):* Figure 5(c) shows that RA reduces the magnitude of human force by 39.4% and 50.3% compared to HL and RL, respectively.

*3) Without obstacles (over the trajectory from L3, L4 to L1):* Figure 5(e) shows that RA reduces the magnitude of human force by 41.9% and 17.5% compared to HL and RL, respectively.

*4) Discussion:* It was realized that the force applied by humans under the RL control strategy is significantly higher than that of RA and HL over the segment of the trajectory with obstacles (i.e. from L1, L2 to L3). This may be related to the human trying to take control to avoid the obstacles, which can be observed in Figure 6.

### B. Average Tracking Error

*1) Over the Whole Trajectory:* Figure 5(b) shows that RA reduces the tracking error by 25.6% compared to HL and increases 7.3% compared to RL.

*2) With obstacles (over the trajectory from L1, L2 to L3):* Figure 5(d) shows that RA reduces the tracking error by 20.5% compared to HL and increases 0.25% compared to RL.

*3) Without obstacles (over the trajectory from L3, L4 to L1):* Figure 5(f) shows that RA reduces the tracking error by 38.8% compared to HL and increases by 39.9% compared to RL.

*4) Discussion:* The tracking error from RL is the smallest because the robot is in control during the experiment and the position of the moving target is known to the robot. However, the obstacle positions are not known to the robot. Therefore, the robot will be likely to move toward the obstacles. This has been shown in table I that RL has the highest failure rate, among the three control strategys, of 40.5%. It can be seen in Figure 6(a), that the variation of the human force in RL is largest compared to HL and RA because the human co-worker needs to apply extraordinary force to take control when closing to the obstacles. Therefore, the gradient of interaction force may be an indicator of whether the human co-worker wants to be in control or signals a low interaction experience.

### C. Failure Rate

TABLE I
FAILURE RATE FOR THE THREE CONTROL STRATEGIES

| Control Strategies | HL | RA | RL |
|---|---|---|---|
| Failure Rate (%) (FR) | 7.4 | 10.7 | 40.5 |

Table I shows the failure rate of the three control strategies. It was realized that the failure rate of RA is similar to HL due to the participant may not pay full attention to the task. And the participants do not become familiar with robots at the beginning and may collide with the obstacles accidentally. When familiarity increases, the failure rate decreases. Moreover, RL is the highest among the three control strategies.

### D. NASA TLX

Figure 7 presents the questionnaire results on perceived workload from the participants based on NASA TLX. NASA TLX is used for participants to provide their feedback. It has six dimensions, including mental demand, physical demand, temporal demand, performance, effort and frustration.

It can be observed that RA is the lowest and RL is the highest in all the six dimensions among all the control

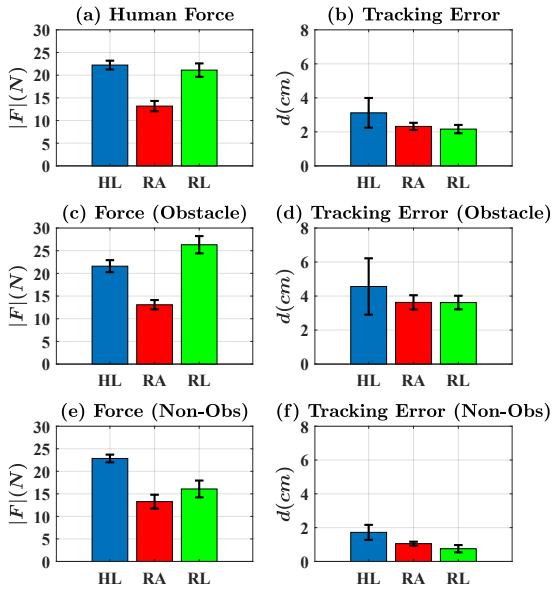


Fig. 5. Evaluations of the three control strategies from the five participants: (a) Human Force (Overall) (b) Tracking Error (Overall) (c) Human Force (Obstacle) (d) Tracking Error (Obstacle) (e) Human Force (Non-obstacles) (f) Tracking Error (Non-obstacle). Obstacles: First half of the trajectory with obstacles, i.e. from L1, L2 to L3. Non-obstacle: Second half of the trajectory without obstacles, i.e. from L3, L4 to L1.

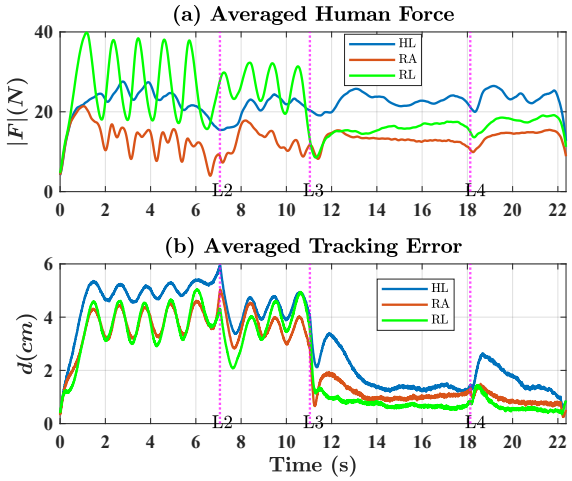


Fig. 6. (a) Averaged Human Force (b) Averaged Tracking Error of the five participants over the experiment at each timestep. The three pink dotted vertical lines are the time step referring to L2, L3 and L4 in Figure 4.

strategies. The significant difference between RA and RL is caused by the misleading of the robot when closing to the obstacles, which are reported by the participants. Therefore, the interaction experience is significantly reduced due to the considerable conflict between humans and robots when closing to the obstacles. An interesting result is that the perceived physical demand is the largest in RL as shown in Figure 7(b). However, human forces of HL are the highest (Figure 5(a)). Consequently, perceived physical demand is not only affected by the objective physical demand applied to the robot, but may also be mental and frustration levels. When the frustration and mental demand are high, the perceived physical demand may also increase correspondingly. This can be an interesting research direction that can be investigated further in the future.

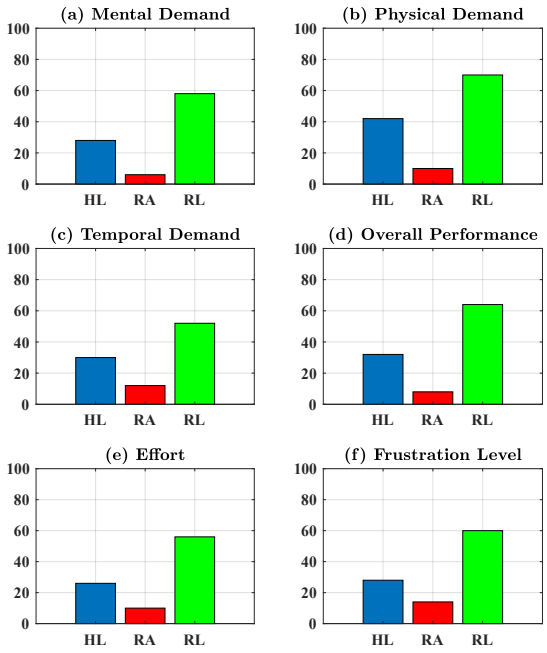


Fig. 7. Normalized subjective results from NASA-TLX from the five participants. 0 - good performance, 100 - bad performance.

## VII. CONCLUSIONS AND FUTURE WORK

We proposed and experimentally verified a TSC-based role arbitration method with human subjects experiment. It has been shown that the proposed role arbitration method could achieve superior human-robot combined performance, reduce human co-workers' workload, and improve subjective preference.

A limitation of the presented work is the small number of participants in this preliminary study. Future works should increase the participant size. A larger participant size is also required to facilitate a rigorous comparison between other frameworks, such as those proposed in [6].

During the experiment, it was observed that different participants, such as different personal qualities and competency levels, had different expectations of the interaction experience with the robot. Therefore, the proposed role arbitration method could also incorporate individual differences, such as personal qualities and competency levels can be another research question to be investigated in the future.

## ACKNOWLEDGMENT

This study is supported in part by the Australian Research Council (ARC) Discovery Project Grant [DP210101093]. The authors would like to thank Jonathan Woolfrey, Yujun Lai and Tiancheng Li for their assistance.

## REFERENCES


[1] H. Yu, S. Huang, G. Chen, Y. Pan, and Z. Guo, "Human-robot interaction control of rehabilitation robots with series elastic actuators," *IEEE Transactions on Robotics*, vol. 31, pp. 1089–1100, 2015.

[2] E. Gambao, M. Hernando, and D. Surdilovic, "A new generation of collaborative robots for material handling," *2012 Proceedings of the 29th International Symposium of Automation and Robotics in Construction, ISARC 2012*, 2012.

[3] S. Aldini, A. Akella, A. K. Singh, Y. K. Wang, M. Carmichael, D. Liu, and C. T. Lin, "Effect of mechanical resistance on cognitive conflict in physical human-robot collaboration," *Proceedings - IEEE International Conference on Robotics and Automation*, vol. 2019-May, pp. 6137–6143, 2019.

[4] D. P. Losey, C. G. McDonald, E. Battaglia, and M. K. O'Malley, "A review of intent detection, arbitration, and communication aspects of shared control for physical human–robot interaction," 2018.

[5] S. Lewandowsky, M. Mundy, and G. Tan, "The dynamics of trust: Comparing humans to automation," *Journal of experimental psychology. Applied*, vol. 6, pp. 104–23, 07 2000.

[6] H. Saeidi and Y. Wang, "Incorporating trust and self-confidence analysis in the guidance and control of (semi)autonomous mobile robotic systems," *IEEE Robotics and Automation Letters*, vol. PP, pp. 1–1, 12 2018.

[7] H. Saeidi, J. R. Wagner, and Y. Wang, "A mixed-initiative haptic teleoperation strategy for mobile robotic systems based on bidirectional computational trust analysis," *IEEE Transactions on Robotics*, vol. 33, no. 6, pp. 1500–1507, 2017.

[8] M. G. Carmichael, R. Khonasty, S. Aldini, and D. Liu, "Human preferences in using damping to manage singularities during physical human-robot collaboration," in *2020 IEEE International Conference on Robotics and Automation (ICRA)*, pp. 10184–10190, 2020.

[9] Q. Wang, D. Liu, M. Carmichael, S. Aldini, and C.-T. Lin, "Computational model of robot trust in human co-worker for physical human-robot collaboration," *IEEE Robotics and Automation Letters*, pp. 1–1, 2022.

[10] P. Evrard and A. Kheddar, "Homotopy switching model for dyad haptic interaction in physical collaborative tasks homotopy switching model for dyad haptic interaction in physical collaborative tasks. whc'09: World haptics-3rd joint eurohaptics conference and symposium on haptic interfaces for virtual environment and teleoperator systems homotopy switching model for dyad haptic interaction in physical collaborative tasks," 2009.

[11] M. G. Carmichael, D. Liu, and K. J. Waldron, "A framework for singularity-robust manipulator control during physical human-robot interaction," *International Journal of Robotics Research*, 2017.

[12] P. A. Hancock, D. R. Billings, K. E. Schaefer, J. Y. Chen, E. J. De Visser, and R. Parasuraman, "A meta-analysis of factors affecting trust in human-robot interaction," *Human Factors*, vol. 53, no. 5, pp. 517–527, 2011.

[13] J. Lee and N. Moray, "Trust, control strategies and allocation of function in human-machine systems," *Ergonomics*, vol. 35, no. 10, pp. 1243–1270, 1992.

[14] B. Navarro, A. Cherubini, A. Fonte, G. Poisson, and P. Fraisse, "A framework for intuitive collaboration with a mobile manipulator," pp. 6293–6298, 09 2017.

[15] S. K. Card, T. P. Moran, and A. Newell, *The psychology of human-computer interaction*. Crc Press, 2018.

[16] M. G. Carmichael, S. Aldini, R. Khonasty, A. Tran, C. Reeks, D. Liu, K. J. Waldron, and G. Dissanayake, "The anbot: An intelligent robotic co-worker for industrial abrasive blasting," *IEEE International Conference on Intelligent Robots and Systems*, pp. 8026–8033, 2019.